Updated Astrometric Measurements of Six Double Stars

Chase Fluegge[1], Alec Remai[2], Robbie Edwards[2], Maïa Villemin[2], Alan Fogel[2], Zach Uchacz [2], Daryl Janzen[2], Rielly Castle[2]
[1] University of Saskatchewan, Saskatoon, Saskatchewan; flueggech2004@gmail.com
[2] University of Saskatchewan, Saskatoon, Saskatchewan

Abstract

This paper presents updated measurements of six double stars and puts forth analysis on the physical relationship of each pair. We have compared historical data to our measurements and checked for patterns that indicate physical relation when graphed, along with calculating physical qualities like escape velocity and the motion of each star through space. Our analysis of WDS 09234-0503/GIC 85, WDS 10159-062/J 3320, WDS 06049-0243/STF 839, WDS 07001-4026/KPP 1112, WDS 09271-1716/SKI 6, and WDS 07072+3401/TVB 152 indicated that all six systems appear to be physically related based on Gaia astrometry. Two systems (SKI 6, STF 838) are likely gravitationally bound, one system (J 3320) is likely not gravitationally bound, and two systems (GIC 85 and TVB 152) were not ruled out as potential binary systems.

1. Introduction

The study of double star systems has long been a fascinating area of research in astronomy, providing valuable insights into stellar dynamics, formation processes, and evolutionary paths. In this paper, we present updated astrometric measurements of six possible double star pairs located in various regions of the sky, though all were observed in the southern hemisphere. The selection of these double star pairs was made following several criteria aimed at increasing the system's scientific interest and relevance. We prioritized systems exhibiting characteristics such as significant proper motion, parallax, or angular separation, as these parameters often indicate potential physical association or gravitational binding between stars. To determine the types of stars comprising each double star pair, we relied on Gaia's HR Diagram (Gaia Collaboration 2019). Our mass estimates were initially based on established relationships between spectral type, luminosity, and mass. However, to ensure accuracy, we cross-referenced our calculations with data from previous studies. Utilizing the Simbad database, we searched for our stars to validate and update our mass estimates, as well as to gather additional insights into their physical characteristics.

GIC 85, J 3320, KPP 1112, and TVB 152 do not appear in SIMBAD, but past astronomical investigations have proposed that both STF 839 and SKI 6 are likely to be wide binary systems (Andrews et al., 2017).

2. Instruments Used

The telescopes used for measurements in this paper are Prompt 5 and PROMPT-MO-1. The former has an aperture of 0.4 m and a focal length of 4576.0 mm. The CCD (charge-coupled device) resolution is 1024 by 1024 pixels and the FOV (field of view) is 10.0 by 10.0 arcmins. It is located at the Cerro Tololo Inter-American Observatory in Chile at an elevation of 2286 meters and is one of eight telescopes available to Skynet at this location. The latter telescope is the only Skynet telescope located at the Meckering Observatory in Australia at an elevation of 197 meters, with an aperture of 0.4 m, a focal length of 4477.0 mm, a CCD resolution of 1024 by 1024 pixels, and an FOV of 10.2 by 10.2 arcmins.

3. Measurement

GIC 85, J 3320, SKI 6, TVB 152, and KPP 112: Using the Skynet telescopes mentioned in the previous section, each pair of stars was imaged and processed in Afterglow. All of these images are clear and without notable defects. Each pair of stars shows clean separation when the images were adjusted for bright objects in Afterglow.
STF 839: This star pair appears to be much closer than the others, but the image does show a clear cutoff after an additional reduction in brightness.

Each of these images could be showing a pair of physically bound stars, but further review indicated that not all of these pairs are bound together.

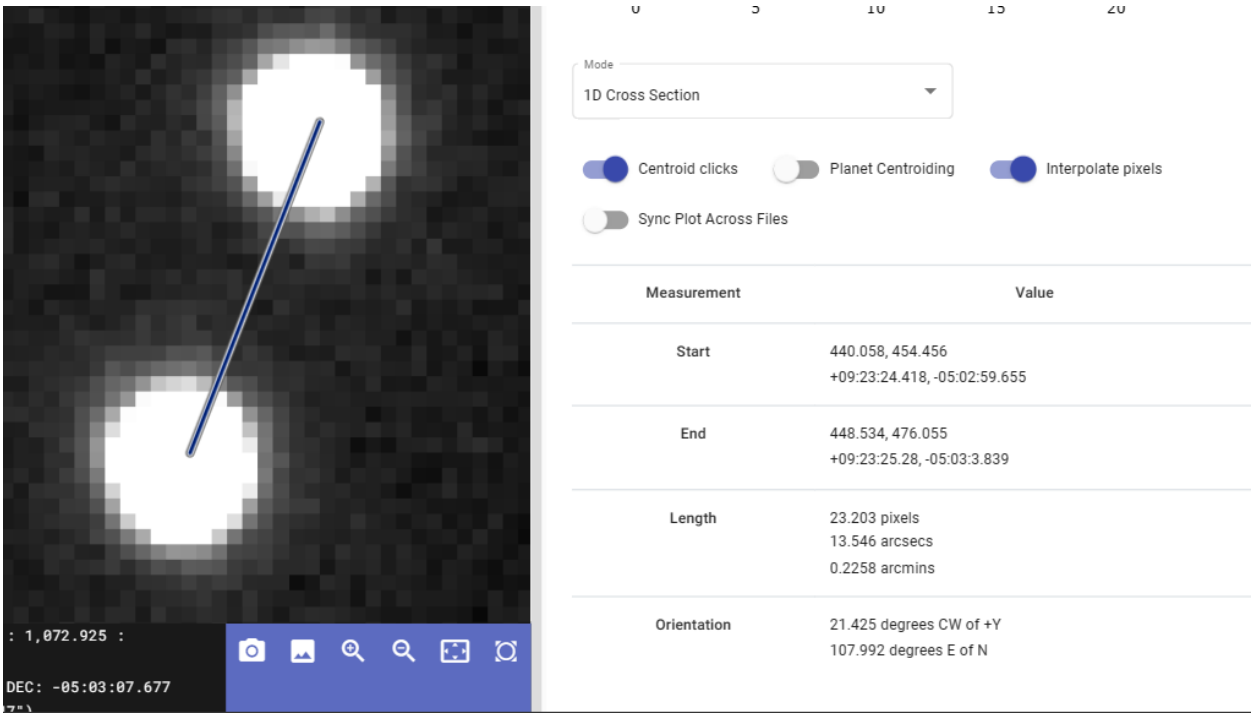

Figure 1: Afterglow measurements of location and orientation of GIC 85

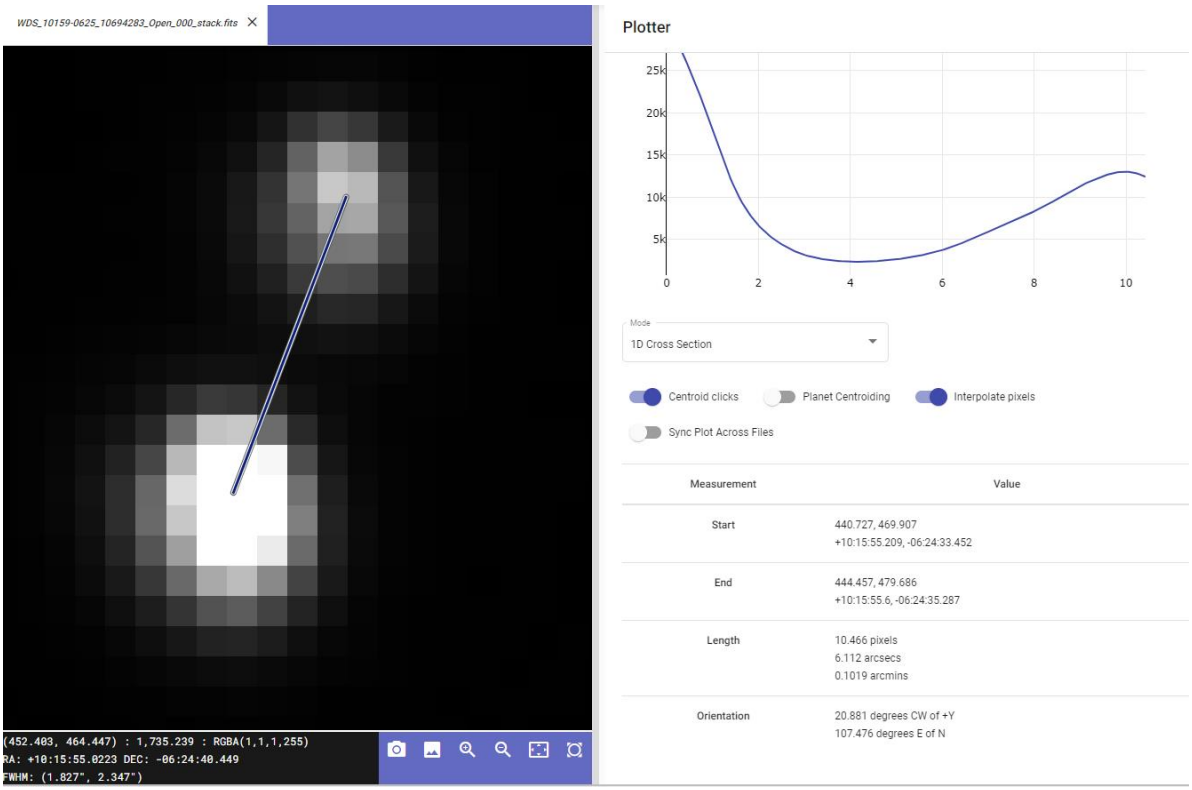

Figure 2: Afterglow measurements of location and orientation of J 3320

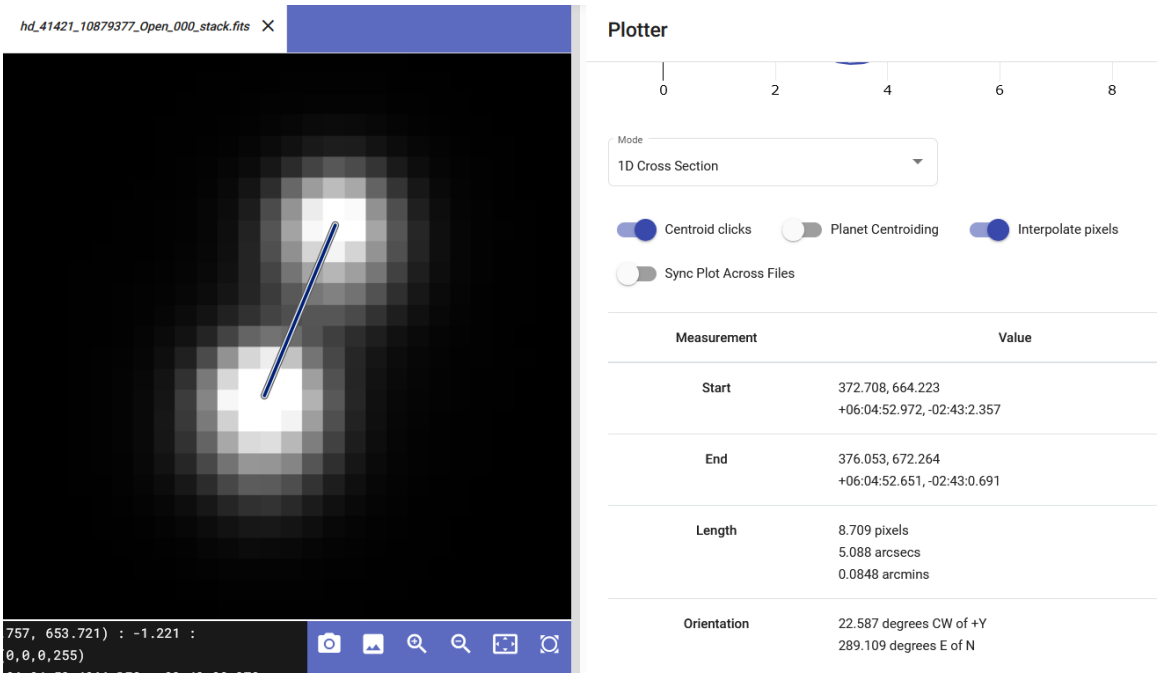

Figure 3: Afterglow measurements of location and orientation of STF839

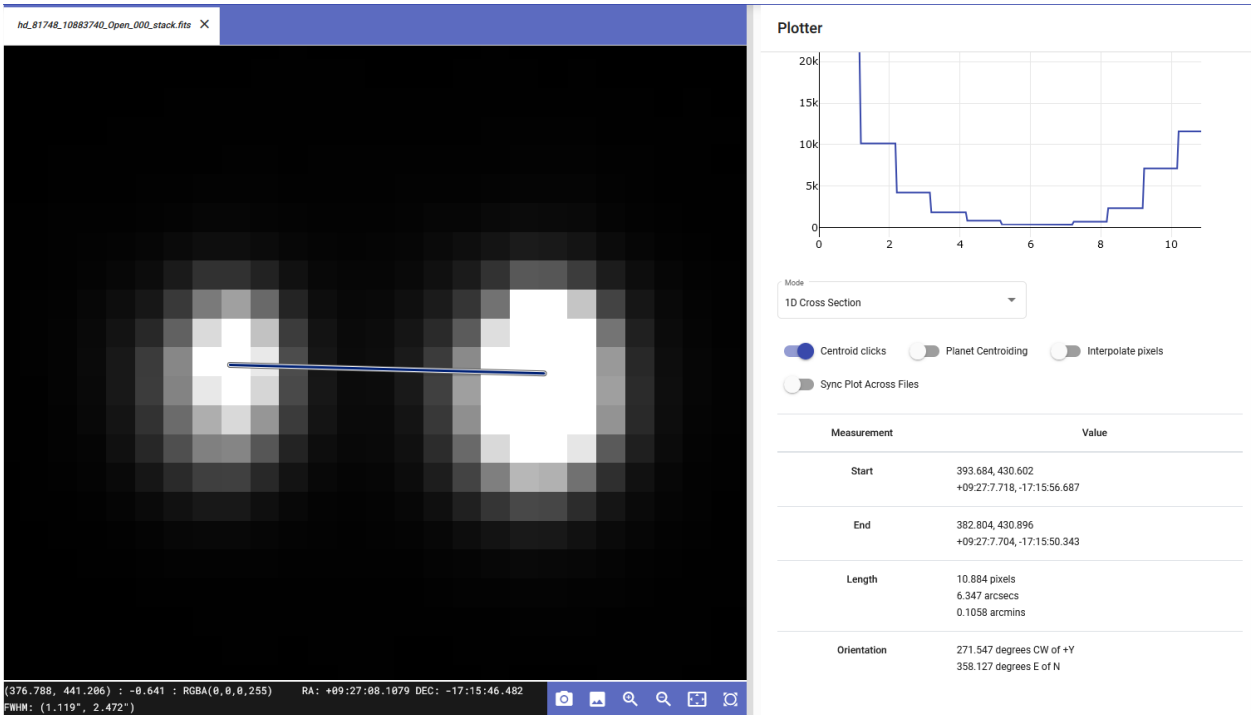

Figure 4: Afterglow measurements of location and orientation of SKI 6

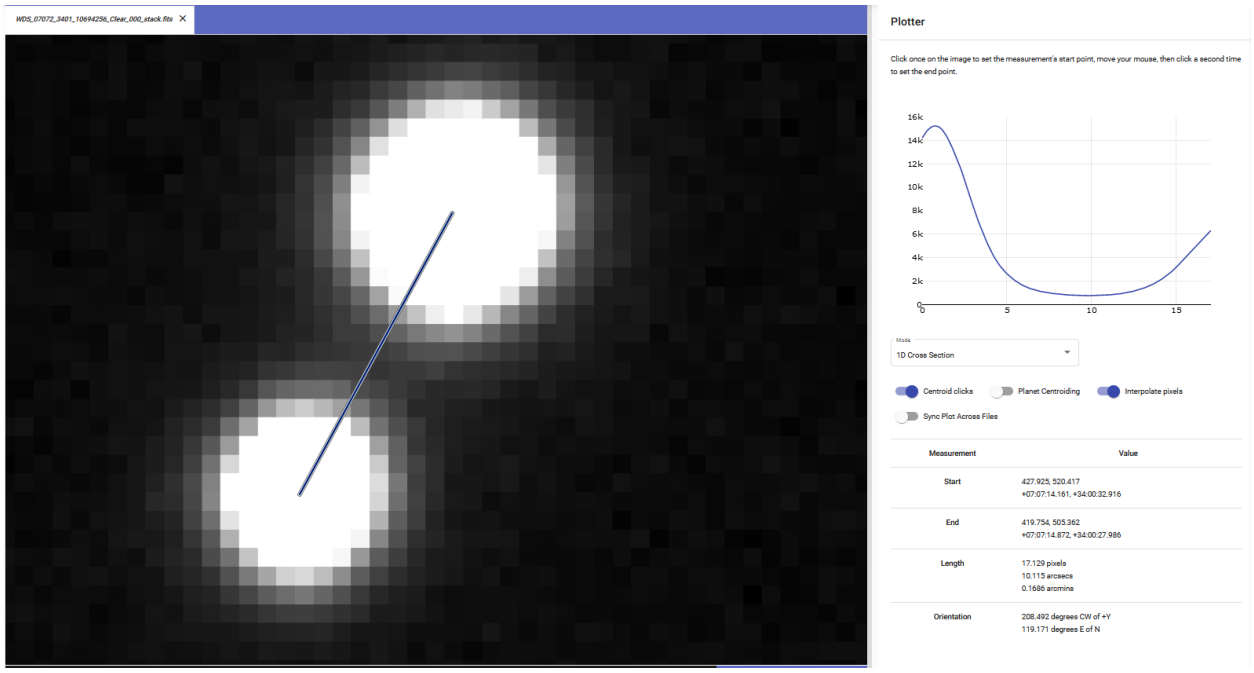

Figure 5: Afterglow measurements of the location and orientation of TVB 152

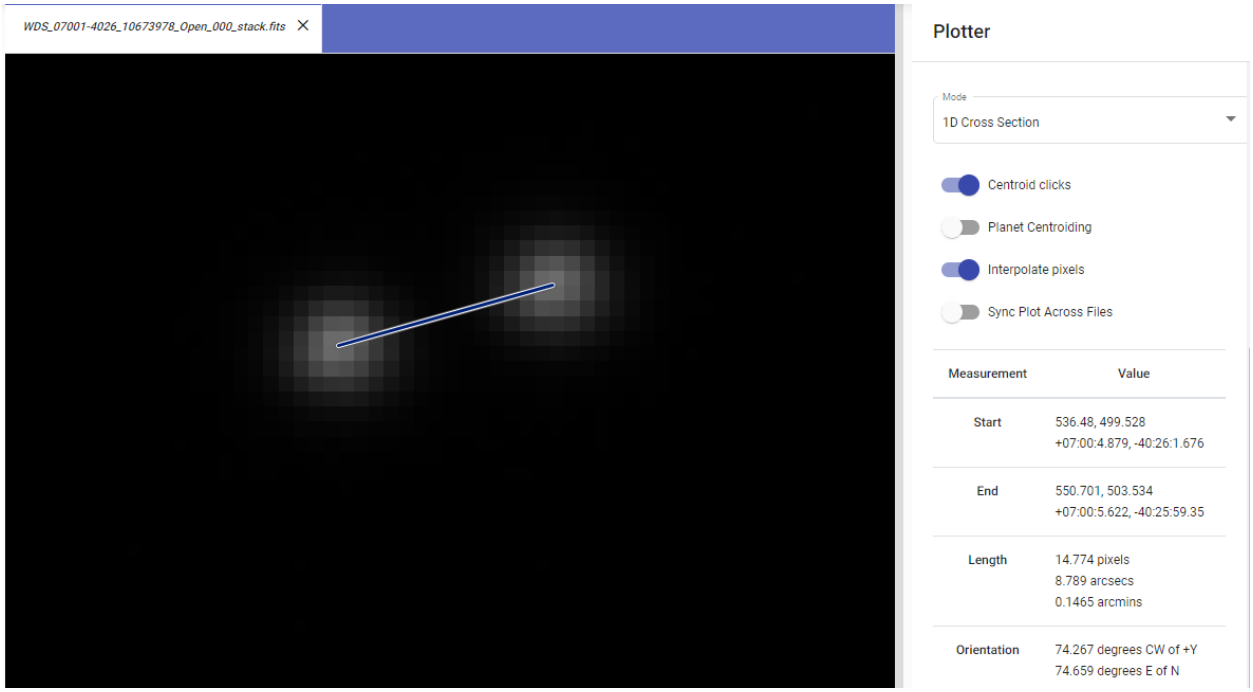

Figure 6: Afterglow measurements for the location and orientation of KPP 112

4. Results

The data in the tables below display the measurements taken of the binary stars. Table 1 summarizes the attributes of each of the observations of the various binary star systems including the relative position angle of the secondary star, the separation between the two stars, and the corresponding error estimates. In all cases, 10 images were taken of each star system.

Table 2 shows Gaia DR3 data for each of the star systems including the parallax and proper motion of each star in each system, and an rPM value (Prusti et al., 2018; Vallenari et al., 2022). The rPM metric reflects the extent to which stars are moving together as calculated by taking the quotient of the relative proper motion of the stars and the longer of the two proper motion vectors. For example, if the two stars are moving identically, then the relative motion is zero, and the quotient is of course zero. There are three classifications for the relationship of the stars based on the quotient. If the resulting quotient is between 0 and 20%, they are classified as a Common Proper Motion pair; if the resulting quotient is between 20% and 60%, they are classed as a Similar Proper Motion pair; and if the resulting quotient is greater than 60%, they are classed as a Different Proper Motion pair (Harshaw, 2016).

Table 3 includes the Relative 3d Space Velocity and the calculated Escape Velocity (Bonifacio et al.)

Table 1. Summary of Measurements.

System	Date	Number of Images	Position Angle (º)	Standard error of Position Angle	Separation (")	Standard Error of Separation
WDS 09234-0503	2024.0792	10	108.0	0.13	13.60	0.020
WDS 10159-0625	2024.0769	10	107.4	0.14	6.13	0.014
WDS 06049-0243	2024.1653	10	288.1	0.09	5.05	0.007
WDS 07001-4026	2024.0669	10	74.6	0.06	8.78	0.014
WDS 09271-1716	2024.0874	10	357.9	0.15	6.4	0.011
WDS 07072+3401	2024.0806	10	119.000	0.03	10.1	0.018

Table 2. Gaia Data.

System	Parallax of Primary (mas)	Parallax of Secondary (mas)	Proper Motion of Primary (mas/yr)	Proper Motion of Secondary (mas/yr)	rPM Quotient	rPM Class
WDS 09234-0503	24.78889	24.7733	-287.54553	-288.68383	0.005	CPM
WDS 10159-0625	3.5941	3.61535	-12.24763	-12.68499	0.018	CPM
WDS 06049-0243	2.25462	2.38061	-3.1116	-3.74393	0.253	SPM
WDS 07001-4026	3.41259	3.3932	-13.9422	-13.57532	0.048	CPM
WDS 09271-1716	8.21626	8.24159	-32.57908	-29.70786	0.074	CPM

WDS 07072+3401	1.516	1.557	-3.443	-3.605	0.036	CPM

Table 3. Proper Motion and Escape Velocity.

	GIC 85	J 3320	STF 839	KPP 1112	SKI 6	TVB 152
Relative 3d Space Velocity (m/s)	280.6	1834.5	3576.4	4902.9	1660.0	911.7
Escape Velocity (m/s) (Bonifacio et al.)	449.7	1398.0	1633.1	1042.7	220.0	32.0

Tables 1 and 2 suggest that many of these systems could be physically bound due to similar Gaia data and physical measurements, with only STF 839 having an rPM class other than CPM. However, Table 3 rules out all but GIC 85.

5. Plots

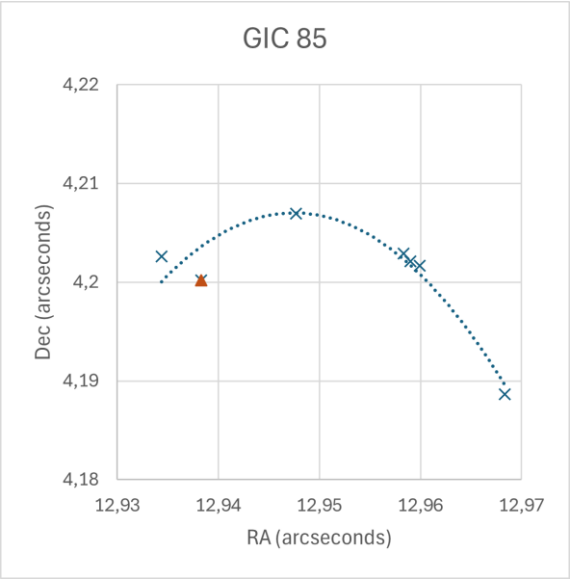

Figure 7: Graph of GIC 85

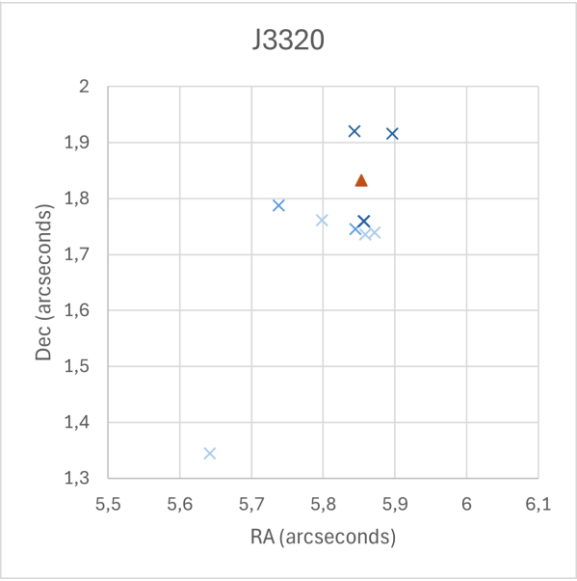

Figure 8: Graph of J 3320

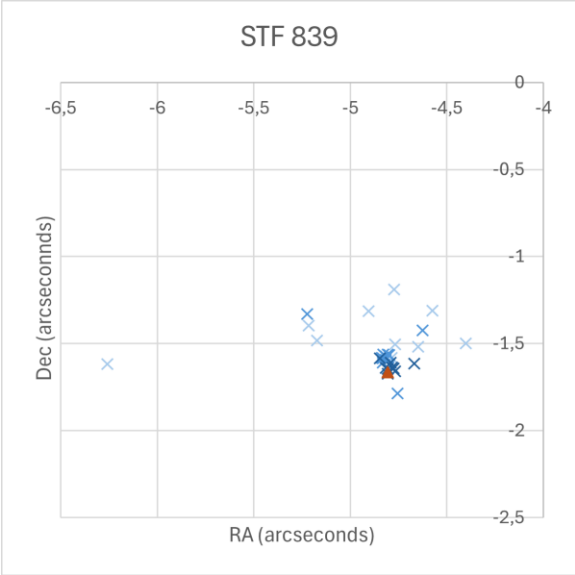

Figure 9: Graph of STF 839

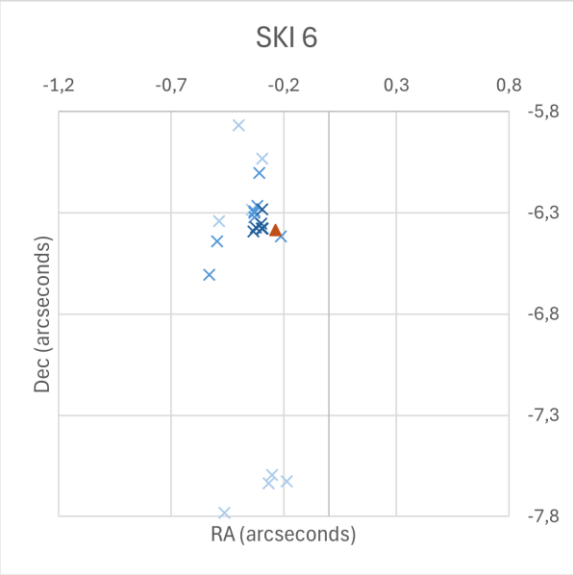

Figure 10: Graph of SKI 6

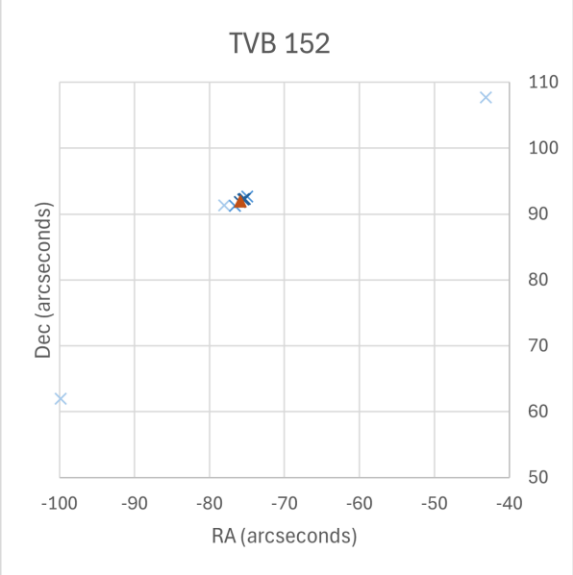

Figure 11: Graph of TVB 152

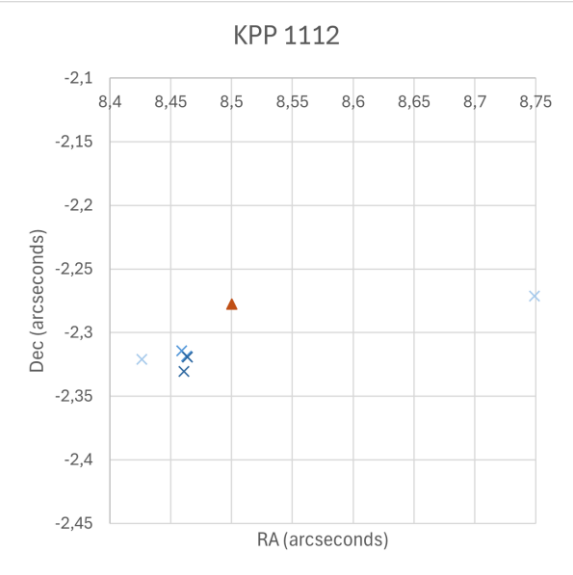

Figure 12: Graph of KPP 1112

Of these systems, there are no existing orbital or linear solutions present in the Sixth Catalog of Orbits of Visual Binary Stars: Orbital Elements.

6. Conclusion

In all cases, the measurements made for these star systems align well with historical observations. The polynomial regression displayed in Figure 7 shows curvature that could be representative of a binary system. As stated in Section 4, these two stars are very similar in their physical qualities, motion through

space, and location. Based on this, it is hard to rule out a physical binary. For J 3320, there is a distinct trend in the data shown in Figure 8, moving upwards and to the right, but there is a lack of curvature. In fact, regression analysis of the plot shows a curvature path down and to the right which is nonsensical for binary orbit given the secondary star is in the positive quadrant. It is more likely the stars are moving past each other given the linear path of the secondary star relative to the first. This also aligns with the conclusion for this system that the stars are not bound because their relative 3D motion exceeds their system escape velocity. There does not seem to be any trend over time regarding STF 839. As seen in Figure 9, there is no linear trend that shows the secondary star moving away from the primary nor a curved path down and left that would indicate that the secondary star is in orbit around the primary star. According to their similar parallax, their rPM quotient, and their small separation, it is more likely that these stars are not bound together but have a similar trajectory in space. There appears to be a trend of the secondary star moving downward away from the primary star in SKI 6 as shown in Figure 10. This reinforces the idea that the stars are not physical binaries. TBV 152 is a compelling example of a physically bound double star system due to physical similarities, but the 3d proper motion and escape velocity listed in Table 3 indicates that this system is not gravitationally bound. There is little historical data to look at for KPP 1112, but the new measurement is within an acceptable margin of error of the few existing measurements shown in Figure 12. The stars are nearly identical in terms of magnitude and motion but are not within escape velocity.

Additional measurements are necessary to further confirm or refute the nature of these systems, especially with more modern means than that of the historical data, some being less accurate than others due to technological limitations. As astronomy progresses through advancements in data collection along with having more opportunities to update measurements throughout the future, the true natures of these systems will be possible to identify with a much higher level of certainty.

Acknowledgements

This research was made possible by the Washington Double Star catalog maintained by the U.S. Naval Observatory, the Stelledoppie catalog maintained by Gianluca Sordiglioni, Astrometry.net, and Skynet Afterglow Access software which was written by Joshua Haislip, Vladimir Kouprianov, and Daniel Reichart. We would also like to extend additional gratitude to Daniel Reichart for his tutorials on Skynet observations and Afterglow Access.
This work has also made use of data from the European Space Agency (ESA) mission Gaia (https://www.cosmos.esa.int/gaia), processed by the Gaia Data Processing and Analysis Consortium (DPAC, https://www.cosmos.esa.int/web/gaia/dpac/consortium). Funding for the DPAC has been provided by national institutions, in particular, the institutions participating in the Gaia Multilateral Agreement.
This work makes use of observations taken by the 0.4m Prompt5 and PROMPT-MO-1 telescopes of the Skynet Robotic Telescope Network located in Cerro Tololo, Chile, and Meckering, Australia, respectively.

References

Andrews, J., J. Chanamé, M. Augüeros. (2017). Wide binaries in Tycho-*Gaia*: search method and the distribution of orbital separations. Monthly Notices of the Royal Astronomical Society, 472(1), 675-699. https://doi.org/10.1093/mnras/stx2000

Bonifacio, B., C. Marchetti, R. Caputo, and K. Tock. (2020). Measurements of Neglected Double Stars. Journal of Double Star Observations, 16(5), 411–423. http://www.jdso.org/volume16/number5/Bonifacio_411_423.pdf

Gaia Collaboration, T. Prusti, J.H.J. de Bruijne, et al. (2016b). The Gaia mission. A&A 595, A1. https://www.aanda.org/articles/aa/full_html/2016/11/aa29272-16/aa29272-16.html

Gaia Collaboration, A. Vallenari, A. G. A. Brown, et al. (2022k). Gaia Data Release 3: Summary of the content and survey properties. arXiv e-prints, https://arxiv.org/abs/2208.00211

Gaia Collaboration (2019). Gaia's Hertzsprung-Russell Diagram. https://sci.esa.int/web/gaia/-/60198-gaia-hertzsprung-russell-diagram

Harshaw, Richard (2016). CCD Measurements of 141 Proper Motion Stars: The Autumn 2015 Observing Program at the Brilliant Sky Observatory, Part 3. Journal of Double Star Observations, 12(4), 394–399. http://www.jdso.org/volume12/number4/Harshaw_394_399.pdf